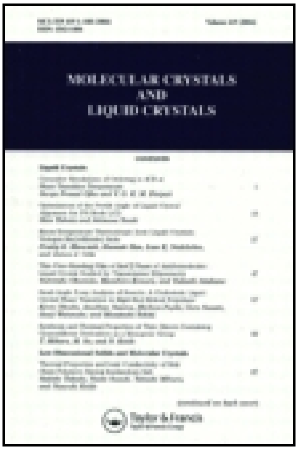

Molecular Crystals and Liquid Crystals Science and Technology. Section A. Molecular Crystals and Liquid Crystals

Publication details, including instructions for authors and subscription information:
http://www.tandfonline.com/loi/gmcl19

Microstructure-Dependent Photoelectric Properties in Porphyrin LB Films

Mitsuru Yoneyama [a], Akiteru Fujii [a], Shuichi Maeda [a] & Tetsuo Murayama [a]

[a] Mitsubishi Kasei Corporation, Research Center, 1000 Kamoshida-cho, Midori-ku, Yokohama, 227, Japan

Version of record first published: 04 Oct 2006.

To cite this article: Mitsuru Yoneyama, Akiteru Fujii, Shuichi Maeda & Tetsuo Murayama (1992): Microstructure-Dependent Photoelectric Properties in Porphyrin LB Films, Molecular Crystals and Liquid Crystals Science and Technology. Section A. Molecular Crystals and Liquid Crystals, 218:1, 189-194

To link to this article: http://dx.doi.org/10.1080/10587259208047038

Mol. Cryst. Liq. Cryst. 1992, Vol. 218, pp. 189–194
Reprints available directly from the publisher
Photocopying permitted by license only

Printed in the United States of America

MICROSTRUCTURE-DEPENDENT PHOTOELECTRIC PROPERTIES IN PORPHYRIN LB FILMS

MITSURU YONEYAMA, AKITERU FUJII, SHUICHI MAEDA
AND TETSUO MURAYAMA
Mitsubishi Kasei Corporation, Research Center
1000 Kamoshida-cho, Midori-ku, Yokohama 227, Japan

ABSTRACT The microstructure-dependence of photoelectric properties have been studied for Langmuir-Blodgett (LB) films containing 5-(4-N-decylpyridinium)-10,15,20-tri-p-tolyl porphyrin (PyP) and arachidic acid (AA). Two-dimensional distribution profiles of short-circuit photocurrent (Isc) exhibited clear bumps and valleys for the LB films with large PyP or AA domains. The spatial averages of Isc tended to show lower values for smaller domain structures, suggesting a great contribution of carrier recombination at the PyP-AA interface.

INTRODUCTION

Recent progress in fluorescence microscopic studies has uncovered a rich variety of microstructures in Langmuir monolayers formed at the air-water interface. These microstructures are interesting from the viewpoint of fundamental research in physics and chemistry since they help us to gain insight into the nature of phase transition and pattern formation in two-dimensional systems[1-2]. It is also important in practical device applications to perform carefull characterization of structural and functional properties of such microstructures since they construct a basic unit for Langmuir-Blodgett (LB) films, and thus they may directly affect the performance of devices with integrated LB films[3].

We have recently succeeded for the first time in measuring photoelectric properties of an array-like porphyrin domain structures in photovoltaic LB films[4-5]. This paper describes an extension of our photoelectrical characterization to various types of microstructures with a view to obtaining valuable information towards a full understanding of correration between structural and functional properties of LB films.

EXPERIMENTAL

Film-forming materials used were 5-(4-N-decylpyridinium)-10,15,20-tri-p-tolyl porphyrin (PyP) as a photovoltaic dye and arachidic acid (AA) as an insulating cosurfactant. Mixtures of PyP and AA were spread from chloroform solutions onto a water surface (pH7, 30℃) to form mixed monolayers.

Experimental details of the morphological and photoelectrical characterization of the monolayers were reported elsewhere[4-5]. The structure of the sandwich-type cell for photocurrent measurement is illustrated in Fig.1. We used six layers of homogeneously mixed monolayer of 5-[4-(10-carboxydecyloxyphenyl)]-10,15,20-tri-p-tolyl porphyrin and AA (mixing ratio, 1:5) as the covering layer. The role of this covering layer is twofold:(1) it protects the PyP:AA layer from damage during Ag evaporation;(2) it allows us to obtain large and stable photocurrents in a short-circuit state since it contains highly photosensitive porphyrin molecules. Two-dimensional distribution of short-circuit photocurrent (Isc) was measured by scanning a monochromatic light at 430nm, focused to 20μm, across the cell surface.

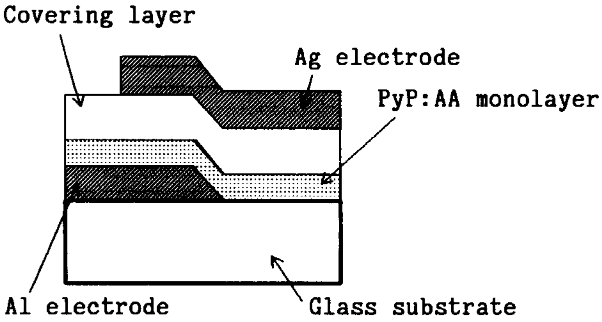

FIGURE 1 Schematic structure of sandwich-type cell.

RESULTS AND DISCUSSION

Typical fluorescence micrographs of the PyP:AA monolayers at 20mN/m are depicted in Fig.2 for various mixing ratios. As-spread monolayers show a distribution of small dark spots due to crystalline

AA domains which are surrounded by fluorescent PyP-dominated region (left column). This configuration is stable with time at low surface pressures (<30mN/m) since the AA domains repel one another due to electrostatic forces arising from a difference in charge density of the solid AA domains and the surrounding fluid phase. However, the texture undergoes a large morphological change through repeated compression and expansion of the monolayer (right column). When the

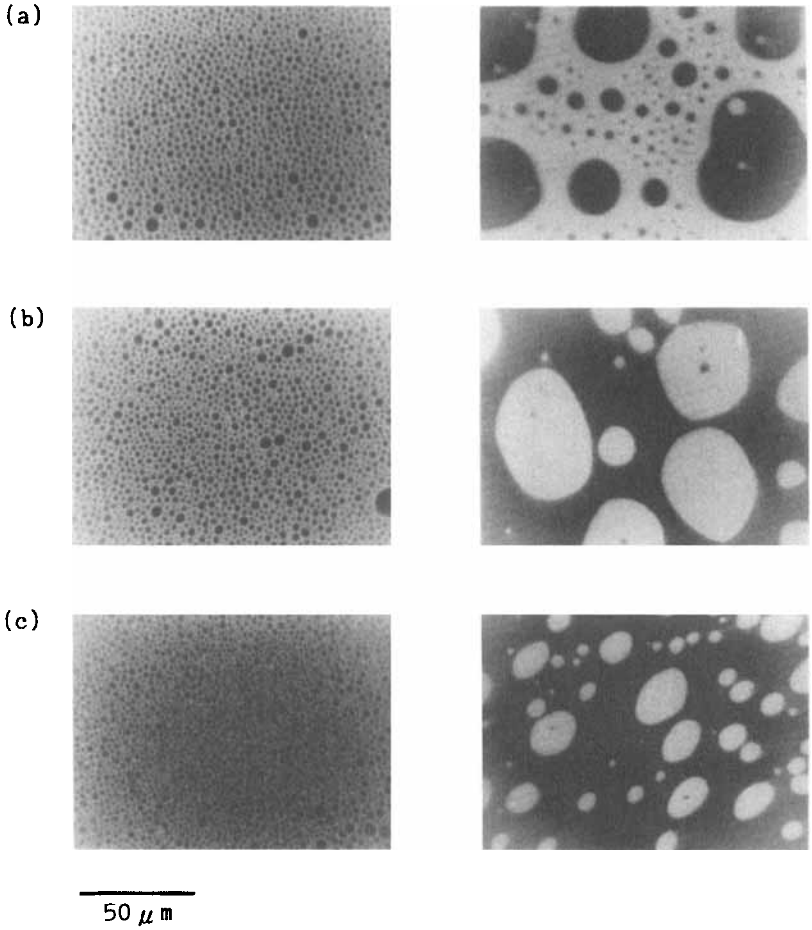

FIGURE 2 Fluorescence micrographs of PyP:AA monolayers with a mixing ratio of 1:5(a), 1:10(b), and 1:20(c). Pictures were taken at 20mN/m immediately after spreading(left column) and after three cycles of compression and expansion(right column).

molar ratio of AA is small (PyP:AA=1:5) the AA domains simply grow in size (Fig.2(a)), whereas at larger AA ratios (1:10 and 1:20) an inversion of domain distribution is observed (Figs.2(b) and 2(c)), *i.e.* PyP forms isolated domains with their average size strongly dependent on the mixing ratio. This change has been previously attributed to the compression-induced merging of AA crystallites[6].

These monolayers were successfully transferred onto solid substrates with their morphologies unaltered, and were incorporated into sandwich-type cells for photoelectrical characterization on the domain level ($\sim 10\,\mu$m). As an example of two-dimensional profiles of Isc, the results for the cells containing 1:10 and 1:5 ratio monolayers are shown in Fig.3. The polarity of the vertical axis is reversed in Fig.3(c). When the cell contains the as-spread PyP:AA

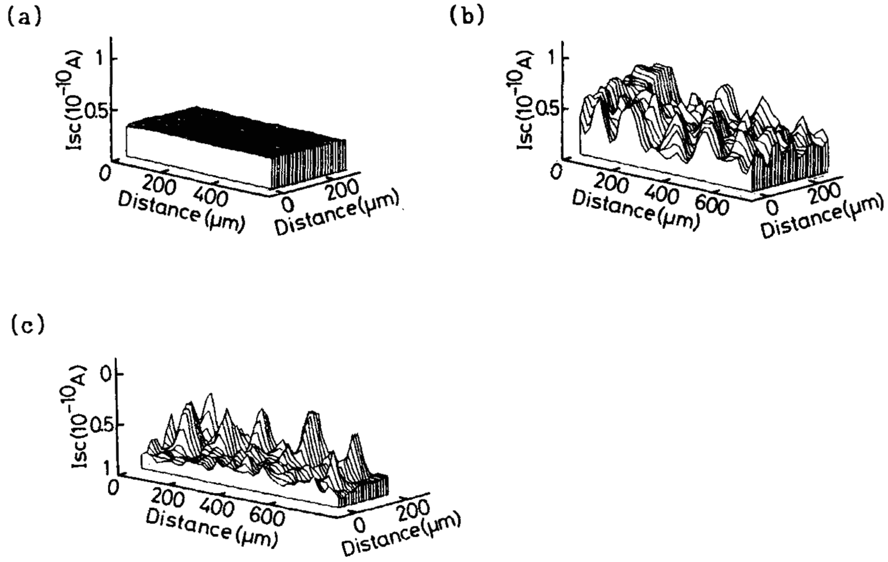

FIGURE 3 Two-dimensional distributions of Isc for sandwich-type cells. (a) PyP:AA=1:10, as-deposited sample; (b) PyP:AA=1:10, cycled sample; (c) PyP:AA=1:5, cycled sample.

monolayer (as-deposited sample), the Isc is almost constant over the whole region investigated (Fig.3(a)), reflecting the uniform distribution of PyP. In contrast, bumps and valleys are found to periodically appear when the PyP:AA monolayer is incorporated after cyclic treatment of compression and expansion (cycled sample, Figs.3(b) and 3(c)). Considering their size and frequency, the bumps in Figs.3(b) and 3(c) are safely regarded as corresponding to large PyP and AA domains, respectively, as seen in Figs.2(b) and 2(a). These results clearly demonstrate that the microscopic distribution of photovoltaic PyP molecules are exactly imaged in the profiles of photocurrent distribution.

Another interesting feature can be noticed if we take out typical cross sections from the two-dimensional profiles and compare

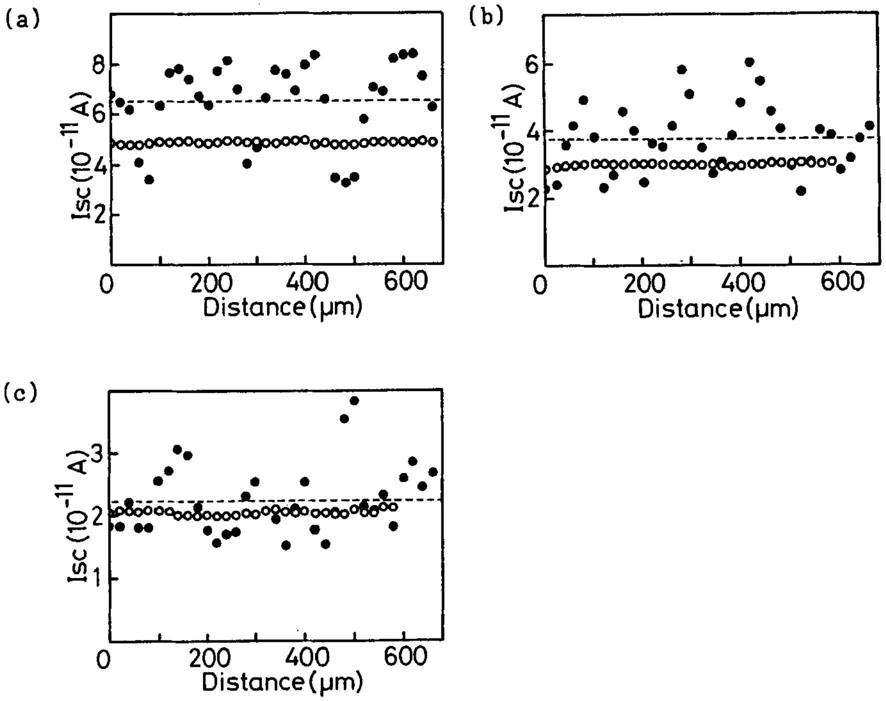

FIGURE 4 Comparison of Isc for as-deposited samples(○) and cycled samples(●) with PyP:AA=1:5(a), 1:10(b), and 1:20(c). Spatial averages of filled dots are indicated by broken line.

the spatial averages of Isc for cycled sample and as-deposited sample at the same PyP:AA mixing raio. A series of such comparison is illustrated in Fig.4. Obviously in all cases the average values of Isc for cycled samples(●), which are indicated by broken line, are larger than those of Isc for as-deposited samples(○). This finding suggests that the photoconductivity in the PyP:AA layer is influenced by its morphology when the dimension of illuminated area is comparable to characteristic domain size. One possible explanation may be that the carrier recombination at the PyP-AA interface becomes less important for cycled samples since the perimeter-to-area ratio is lower with larger domains, thus leading to higher photocurrents. According to this mechanism, the difference in average Isc between the two types of samples is expected to diminish with increasing beam diameter because the contribution of charge recombination at the domain periphery becomes negligible compared with the total carriers photogenerated in the illuminated area. Actually, morphology-independent photocurrents were obtained by illuminating an area of about 1-cm diameter on the cell surface.

ACKNOWLEDGMENT

This work was performed under the management of FED (the R&D Association for Future Electron Devices) as a part of the R&D of Basic Technology for Future Industries supported by NEDO (New Energy and Industrial Technology Development Organization).

REFERENCES

1. C. M. Knobler, Science, 249, 870 (1990).
2. J. Prost and F. Rondelez, Supplement to Nature, 350, 18 (1991).
3. C. Duschl, D. Kemper, W. Frey, P. Meller, H. Ringsdorf, and W. Knoll, J. Phys. Chem., 93, 4587 (1989).
4. M. Yoneyama, A. Fujii, S. Maeda, and T. Murayama, Appl. Phys. Lett., 58, 2381 (1991).
5. M. Yoneyama, A. Fujii, S. Maeda, and T. Murayama, Thin Solid Films, submitted for publication.
6. M. Yoneyama, A. Fujii, S. Maeda, and T. Murayama, Chem. Lett., 929 (1991).